Heat and Mass Transfer 39 (2003) 869–876
DOI 10.1007/s00231-003-0413-4

An experimental investigation of the combined effects of surface curvature and streamwise pressure gradients both in laminar and turbulent flows

A.A. Ozalp, H. Umur

Abstract Flow and heat transfer characteristics over flat, concave and convex surfaces have been investigated in a low speed wind tunnel in the presence of adverse and favourable pressure gradients (k), for a range of $-3.6 \times 10^{-6} \leq k \leq +3.6 \times 10^{-6}$. The laminar near zero pressure gradient flow, with an initial momentum thickness Reynolds number of 200, showed that concave wall boundary layer was thinner and heat transfer coefficients were almost 2 fold of flat plate values. Whereas for the same flow condition, thicker boundary layer and 35% less heat transfer coefficients of the convex wall were recorded with an earlier transition. Accelerating laminar flows caused also thinner boundary layers and an augmentation in heat transfer values by 28%, 35% and 16% for the flat, concave and convex walls at $k = 3.6 \times 10^{-6}$. On the other hand decelerating laminar flows increased the boundary layer thickness and reduced Stanton numbers by 31%, 26% and 22% on the flat surface, concave and convex walls respectively. Turbulent flow measurements at k = 0, with an initial momentum thickness Reynolds number of 1100, resulted in 30% higher and 25% lower Stanton numbers on concave and convex walls, comparing to flat plate values. Moreover the accelerating turbulent flow of $k = 0.6 \times 10^{-6}$ brought about 29%, 30% and 24% higher Stanton numbers for the flat, concave and convex walls and the decelerating turbulent flow of $k = -0.6 \times 10^{-6}$ caused St to decrease up to 27%, 25% and 29% for the same surfaces respectively comparing to zero pressure gradient values. An empirical equation was also developed and successfully applied, for the estimation of Stanton number under the influence of pressure gradients, with an accuracy of better than 4%.

List of Symbols

C_p	constant pressure specific heat, J/kgK
C_f	skin friction factor, dimensionless
h	convective heat transfer coefficient, W/m^2K
H	shape factor
k	pressure gradient parameter $[(\nu/U^2)(dU/dx)]$, dimensionless
k_x	streamwise pressure gradient $[(x_p/U)(dU/dx_p)]$, dimensionless
q_F, q_o	flow-on and flow-off powers, W/m^2
Re_x	streamwise distance Reynolds number, dimensionless
Re	momentum thickness Reynolds number, dimensionless
St	Stanton number, dimensionless
St_o	Stanton number without longitudinal pressure gradient, dimensionless
St_p	Stanton number with longitudinal pressure gradient, dimensionless
T_w	wall temperature, °C
T_o	free stream temperature, °C
U	mean velocity, free stream velocity, m/s
x,y,z	streamwise, pitch wise and spanwise directions, mm
x_l	unheated starting length, mm
x_p	pressure imposed streamwise length, mm

Greek Symbols

δ	boundary layer thickness, mm
ν	kinematic viscosity, m^2/s
ρ	density, kg/m^3
θ	momentum thickness, mm

Received: 13 February 2002
Published online: 4 March 2003

A.A. Ozalp, H. Umur (✉)
Department of Mechanical Engineering,
Uludag University 16059 Gorukle Bursa, Turkey
E-mail: umur@uludag.edu.tr
Fax: +90-224-4428899

1 Introduction

Concave and convex surfaces are of great importance for engineering applications such as turbine blades, aircraft wings and power plants, which are bound to adverse and favourable pressure gradients. There have been several previous investigations particularly on flat plate boundary layers and a few in curved walls such as Abu-Ghannam and Shaw [1] who worked on the effects of turbulence intensities and pressure gradients, Crane and Sabzvari [2] who showed that Görtler vortex system due to concave curvature caused St to increase above flat plate values by a comparable amount. Umur [3] showed that pressure gradient parameters up to 0.75×10^{-6} over concave curvature resulted in regular vortex structure and caused mean heat transfer coefficient to increase, and also determined that a value of k of 1.8×10^{-6} was sufficient to suppress the vortex development so that there was no heat transfer augmentation above the flat plate values. Gostelaw et al. [4] determined that transition occurs rapidly under strong adverse pressure gradients, Zhang et al. [5] indicated the late transition character in laminar and turbulent flows over a concave curvature and Zhou and Wang [6] reported the effects of free-stream turbulence intensity and streamwise acceleration on flow and heat transfer. Volino and Simon [7] found out that high free stream turbulence (8%) shortens the transition length but accelerating flow ($k = 9 \times 10^{-6}$) overcomes the effects of turbulence intensity. Umur and Karagoz [8] showed that Stanton numbers increased with favourable pressure gradients and decreased with the adverse in flat plate walls. Sturgis and Mudawar [9] reported that higher Reynolds number caused higher heat transfer rates in the downstream region but lower in the upstream region at the concave wall. Wright and Schobeiri [10] reported that increasing the unsteadiness results in earlier transition and higher heat transfer rates. Umur [11] presented over a concave surface that the effect of Reynolds number on heat transfer enhancement is more dominant than surface curvature and pressure gradients.

A number of investigations have also been carried out in turbulent flows. For example Muck et al. [12] concluded that the response of turbulence to convex curvature is rather rapid and the decrease in turbulence intensity is implied by the increase of turbulent-energy dissipation rate. Wang and Simon [13] reported 5% to 10% decrease in heat transfer due to convex curvature and free-stream turbulence effects became dominant on convex curvature transition and Taylor et al. [14] investigated the flat plate turbulent heat transfer process for two different boundary conditions. Plesniak et al. [15] worked on the effect of angular momentum instability on the mixing layer as the low speed stream is close to or away from the curved wall and Rivir et al. [16] reported that heat transfer rates dropped below the zero pressure gradients by 60% near the separation point but the values rapidly increased when approaching the reattachment point. Inagaki and Aihara [17] determined that the meandering motion of the Görtler vortices, appeared from transition to turbulent regions, was dominant near the wall, contributing to the energy exchange with the turbulence. The friction factor appeared to be most influenced by the decelerating turbulent flows over convex curvatures in the study of Webster et al. [18]. Kestoras and Simon [19] determined that turbulence quantities immediately dropped at the bend exit, while Ligrani and Hedlung [20] showed that concave wall heat transfer rates were above the convex values by 30% to 40% in the transition and turbulent regions respectively.

In this study; flat, concave and convex wall boundary layers have been investigated in conjunction with pressure gradients both in laminar and turbulent flows, so as to determine the combined effects of pressure gradient and wall curvature on the boundary layer development and heat transfer rates. Velocity and temperature measurements were recorded with initial free stream momentum thickness Reynolds numbers ($Re_\theta = U\theta/\nu$) from 200 to 2000 and the pressure gradient parameter of k $[(\nu/U^2)(dU/dx)]$ from -3.6×10^{-6} to $+3.6 \times 10^{-6}$ for laminar and from -0.6×10^{-6} to $+0.6 \times 10^{-6}$ for turbulent flows, corresponding to k_x $[(x_p/U)(dU/dx_p)]$ values of ±0.47.

2
Flow conditions and instrumentation

All measurements were conducted in three rectangular test sections of straight, concave and convex surfaces mounted on a low-speed wind tunnel manufactured at Uludag University as shown in Fig. 1. Air was drawn by a 5 kW centrifugal blower through honeycomb and screen packs with an area constriction of 3 to provide a maximum exit velocity of 30 m/s. A straight plate in 400 mm length was also installed in the upstream of the test section to allow the boundary layer growth at the leading edge. The streamwise distance is 750 mm in straight wall and 1000 mm in curved walls with a radius of 1500 mm either in concave or convex curvatures. Upper walls of three test section were adjustable to impose the desired favourable or adverse constant pressure gradients (k) from -3.6×10^{-6} to $+3.6 \times 10^{-6}$. The highest value of k was close to that required to relaminarise the turbulent boundary layers. The pressure gradient parameter was chosen to characterise acceleration (k=+) and deceleration (k=–) on the basis of ease of measurement and k values were tried to be kept constant from the leading edge to the trailing edge with an accuracy of ±5%. k_x values were also used as a streamwise imposed pressure gradient to simplify the analysis and to compare the measurements of laminar and turbulent flows.

Mean velocities were measured by a semicircular pitot tube, at 6 different streamwise locations of x = 60, 180, 300, 420, 540 and 660 mm, mounted on the lower side of the test section in conjunction with the static pressure tappings. Static pressures were recorded by a micro manometer with a precision of ±1%. The total uncertainty in mean velocity was estimated to be within ±4%. The copper plate test wall was heated by an electrical resistance (a high-current low-voltage transformer) to provide surface temperature measurements under the constant heat flux condition. Wall temperatures were recorded by copper-constantan thermocouples on the heated copper plate mounted either on concave, convex or straight walls. Care was taken to minimise heat loss through the backside of wall by fibreglass insulation. The temperature distribution above all heated walls was found to be uniform in streamwise direction within ±0.5 °C throughout the measurements. Convection heat loss was estimated from the difference between the flow-off (q_o) and flow-on (q_F) powers required to maintain locally constant wall temperature with and without flow. The heat transfer coefficient is defined as $h = q/(T_w - T_o)$ and corresponding experimental Stanton number by $St = h/(\rho U C_p)$ where $q = q_F - q_o$, T_w and T_o are the wall and free stream temperatures, ρ, U and C_p refer to density of fluid, free stream velocity and specific heat.

The boundary layer thickness $\delta_{(0.95U)}$ at the first measuring station (60 mm) of the flat surface was 13 and 10 mm with free stream velocities of 3 m/s (laminar flow) and 15 m/s (turbulent flow) respectively. The corresponding initial values of δ were 11 and 8 mm for concave and 14 and 12 mm for convex surfaces.

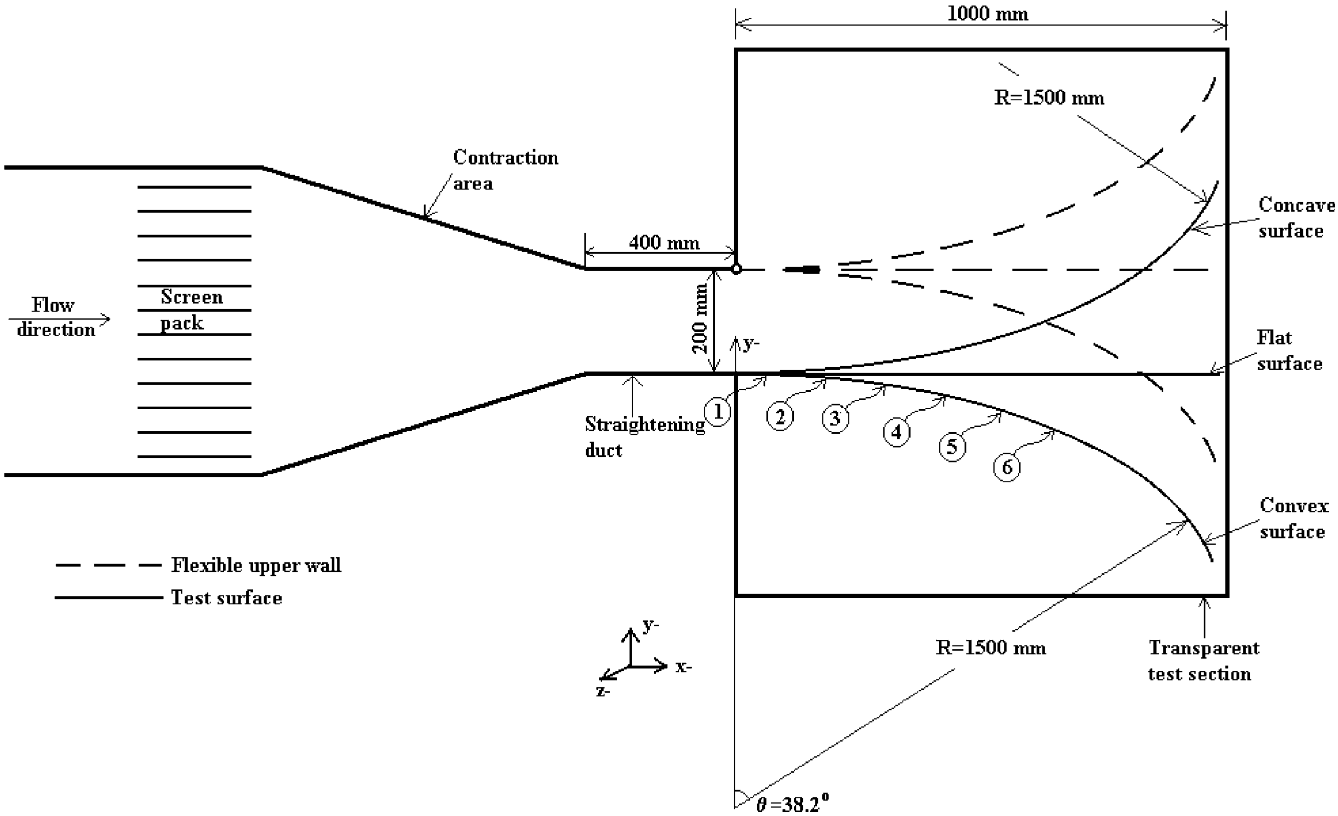

Fig. 1. Test section

3
Results and discussions

Two different inlet velocities of 3 m/s in laminar and 15 m/s in turbulent flows were implied to form a complete overview on flow and heat transfer characteristics on flat, concave and convex surfaces and to set laminar and turbulent flow regimes, with streamwise pressure gradients from -3.6×10^{-6} to $+3.6 \times 10^{-6}$ in laminar flows and from -0.6×10^{-6} to $+0.6 \times 10^{-6}$ in turbulent flows. Velocity and temperature measurements were obtained at 6 locations of the test surfaces and presented as laminar and turbulent flows in cross stream and streamwise variations based on the boundary layer parameters of δ, Re_x, Re_θ, H, C_f and St.

3.1
Laminar accelerating and decelerating flows

Laminar flow experiments are carried out with an inlet velocity of 3 m/s for all surfaces with near zero, favourable and adverse pressure gradients. Although the velocity and heat transfer measurements were carried out at 6 stations in streamwise direction, the non-dimensional velocity profiles of the three surfaces were shown at three locations of 60, 300 and 660 mm, for the sake of brevity only, and for pressure gradients of k = 0 and $\pm 3.6 \times 10^{-6}$, as in Fig. 2. The initial boundary layer thicknesses of the concave, flat and convex surfaces ($\delta_{x\,=\,60mm}$) are 11, 13 and 14 mm which lead to streamwise distance Reynolds numbers ($Re_x = Ux/\nu$) of 175000, 245000 and 285000, Re_θ of 230, 280 and 360 and H of 2.55, 2.75 and 2.95 respectively for all pressure gradients. On the other hand downstream (x = 660 mm) values of Re_θ are evaluated as 420, 480 and 590 and H values appeared to be 1.80, 2.1 and 2.20 for the concave, flat and convex surfaces respectively for near zero pressure gradient. Flat surface boundary layer values match with laminar notifications of Cebeci and Bradshaw [21] and flat plate velocity profiles are similar to that of Cheng et al. [22]. Velocity profiles at the last two stations of the concave surface resemble those of Volino and Simon [7] and Inagaki and Aihara [17] from the point of transition. Whereas, the convex surface flow show laminar flow characteristics all over the surface, similar to those of Plesniak et al. [15]. The velocity profiles of Fig. 2 show that concave curvature enhances the onset of transition, contrary to the convex curvature. Implementation of the favourable pressure gradient of $k = 2.0 \times 10^{-6}$ showed no significant effect on the initial station boundary layer parameters, but thinner boundary layers appeared in the streamwise direction so that boundary layer thicknesses for all three surfaces reduced by 8% at the last station, together with Re_θ values of 350, 440 and 550 and H values of 1.87, 2.15 and 2.25 for concave, flat and convex surfaces respectively. The stabilising effect of acceleration can also be seen for all surfaces, being consistent with the work of Zhang et al. [5]. The similar boundary layer development was also recorded with the highest pressure gradient parameter of $k = 3.6 \times 10^{-6}$, which shows that the highest pressure gradient was not sufficient for the laminar boundary layer development particularly at the initial station. But, the effect of favourable pressure gradient became more remarkable towards the end of test section so that Re_θ and H values for all surfaces became smaller than those of near zero and

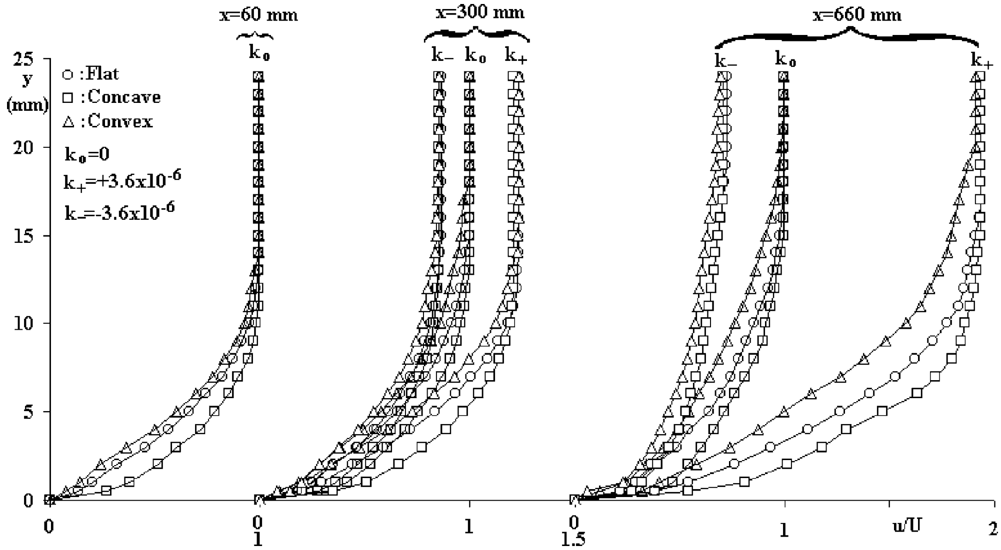

Fig. 2. Streamwise variation of laminar velocity profiles with $k = 0$ and $\pm3.6 \times 10^{-6}$

mild pressure gradient ($k = 2.0 \times 10^{-6}$), which are in conjunction with the flat surface results of Gostelaw et al. [4]. The deviation from core velocity between the first and the last stations is recorded as 20% of the initial free stream velocity for the mild adverse pressure gradient. Deceleration in the streamwise direction brought about thicker boundary layers and earlier transition with higher Re_θ (420, 500 and 595) and H values (1.76, 2.04 and 2.11) than those of accelerating values for concave, flat and convex surfaces respectively. The concave wall boundary layer characteristics are consistent with the values of Volino and Simon [7], who recorded that the onset of transition took place towards the end of concave curvature. Decelerating flows caused thicker boundary layer thickness and corresponding lower C_f values as expected for all cases, contrary to the accelerating flows. The strongest adverse pressure gradient of $k = -3.6 \times 10^{-6}$ was not sufficient to cause inflected velocity profiles at upstream locations, but the laminar velocity profiles appear to be more vulnerable towards the downstream, with a small sign of separation particularly on the convex wall. The measured boundary layer parameters of δ, Re_θ and H are inconsistent with the values of Rivir et al. [16] for the flat surface but consistent with Muck et al. [12] for convex surface and Plesniak et al. [15], who reported the onset of transition at $Re_x = 3.8 \times 10^5$.

Heat transfer measurements have also been simultaneously carried out at the same stations and the measured Stanton numbers of the three surfaces are compared within each other and also with the laminar analytical solution for constant heat flux of Eq. (1)

$$St = 0.453 Re_x^{-0.5} Pr^{2/3} \left(1 - (x_l/x)^{0.75}\right)^{-1/3} \tag{1}$$

where Re_x is the streamwise distance Reynolds number, Pr is the Prandtl number, x_l is the unheated starting length and x is the streamwise distance. As shown in Fig. 3, St decreases in the streamwise direction for all surfaces in the presence of near zero ($k = 0$) and favourable pressure gradients ($k = 2.0$, 3.6×10^{-6}). The higher St on the concave wall and the lower on the convex wall result partly from thinner and thicker boundary layers as

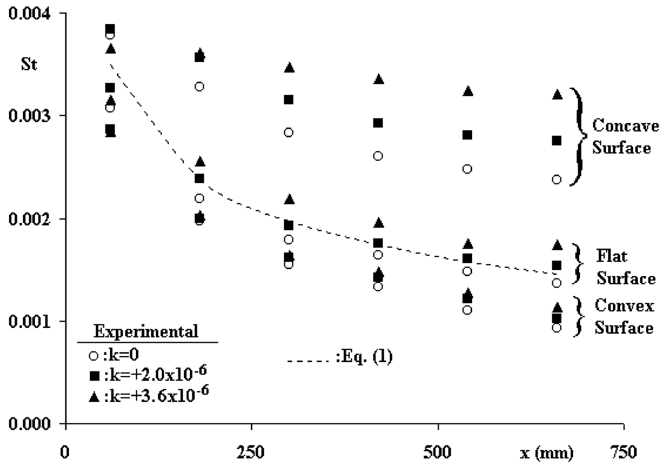

Fig. 3. Streamwise variation of Stanton numbers in laminar flow with favourable pressure gradients

expected and the measured values and analytical solutions (Eq. (1)) of flat surface are very close to each other. The fuller velocity profiles and the higher skin friction coefficient (C_f) on the concave wall gave rise to an augmentation of St by up to 90% towards the end of curvature comparing to those of flat plate values, which are higher than that of Umur [11] and lower than those of Wright and Schobeiri [10]. The thicker boundary layer thickness and lower skin friction on the convex wall, at $k = 0$ flow, caused St to decrease by 35%, which is smaller than those of Turner et al. [23] and is consistent with Wang and Simon [13] who reported higher heat transfer rates on strong convex curvature.

Heat transfer coefficients at $k = 2.0 \times 10^{-6}$ were close to those of near zero pressure gradient at the initial station but increased a considerable amount towards the last station for all surfaces. The effect of favourable pressure gradient on St enhancement was more pronounced on concave surface (16%) than flat surface (13%) and convex surface (5%) comparing to those of zero pressure gradient, which are in accord with the results of Umur and Karagöz [8] and Zhou and Wang [6]. Fig. 3 shows that flat surface St is 78% below that of the concave and 34% above the

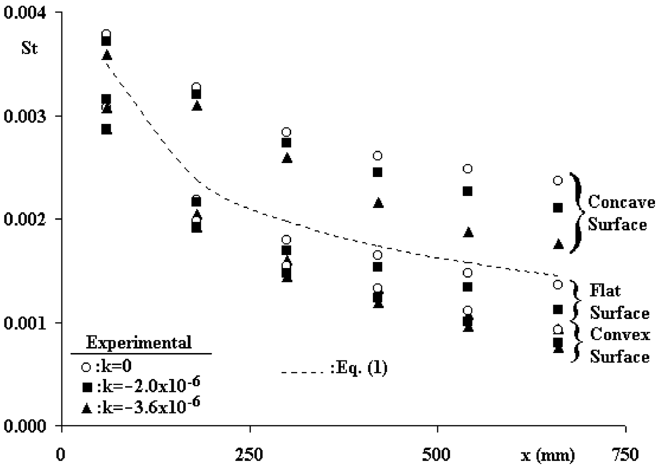

Fig. 4. Streamwise variation of Stanton numbers in laminar flow with adverse pressure gradients

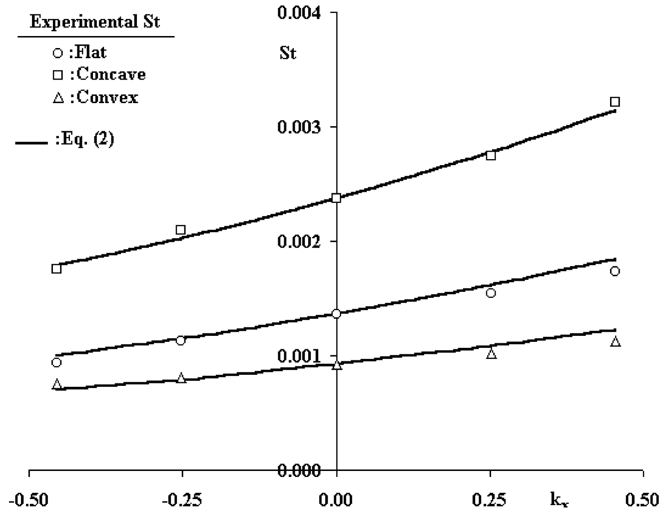

Fig. 5. Laminar flow Stanton numbers versus k_x

convex wall at the last station, similar to those of near zero pressure gradient. The convex curvature St results are inconsistent with Turner et al. [23], who reported 18% increase at $k = 0.15 \times 10^{-6}$.

Moreover the strongest favourable pressure gradient of $k = 3.6 \times 10^{-6}$ caused thinner δ and smaller boundary layer parameters of H and Re_θ, which resulted in higher St in the streamwise direction. Fig. 3 also shows that the heat transfer coefficient in the case of $k = 3.6 \times 10^{-6}$ reached higher values than those of with mild pressure gradient. Furthermore, the augmentation of St in flat surface became apparent with the comparison of the analytical values of Eq. (1). On the other hand concave, flat and convex surface heat transfer rates increased by 35%, 28% and 16% respectively, comparing to those of zero pressure gradient values, which indicates that curvature effects are more dominant than acceleration on Stanton number variation.

Adverse pressure gradient St measurements are shown in Fig. 4 for the three surfaces. Stanton number, in the case of $k = -2.0 \times 10^{-6}$, decreased by 11% on concave and 17% both on flat and convex surfaces, comparing to those of near zero pressure gradient. Flat surface St values remained again above convex and below concave surface values; particularly at the last station with the highest value of 85% and the lowest value of 30% respectively. These measurements prove that convex surface is more vulnerable to adverse pressure gradient and the concave surface overwhelms the opposite effects of adverse pressure gradient.

The strongest adverse pressure gradient of -3.6×10^{-6} resulted in 26%, 31% and 22% lower St values than those of near zero pressure gradient on the concave, flat and convex surfaces respectively, Fig. 4 also displays 88% higher St on concave and 20% lower St on convex surfaces comparing to flat plate values for the $k = -3.6 \times 10^{-6}$ case.

A new equation for the estimation of St as a function of the new pressure gradient parameter of k_x was developed and compared with all measured St for both accelerating and decelerating flows. The new equation is defined as

$$St_p = St_o \exp(0.6k_x) \tag{2}$$

where k_x is the streamwise pressure gradient, St_p and St_o stand for the St values with and without longitudinal pressure gradients. Variation of the experimental Stanton numbers with respect to k_x and Eq. (2) are plotted in Fig. 5, showing that the measured St are very close to the analytical values and lie on the empirical curve.

In the presence of the strongest adverse streamwise pressure gradient of $k_x = -0.47$ ($k = -3.6 \times 10^{-6}$) flat surface St values are above that of the convex by 20% and below concave surface measurements by 88%; whereas these proportions become 35% (flat-convex) and 85% (flat-concave) for the highest favourable streamwise pressure gradient of $k_x = 0.47$ ($k = 3.6 \times 10^{-6}$). Eq. (2) can successfully be used for all surfaces in the pressure gradient range of $-1.0 \leq k_x \leq 1.0$ with a precision of ±3%.

3.2 Turbulent accelerating and decelerating flows

Turbulent flow measurements were carried out at 6 streamwise locations of x = 60, 180, 300, 420, 540 and 660 mm as in the laminar case, with an inlet velocity of 15 m/s and with pressure gradients of $\pm 0.4 \times 10^{-6}$ and $\pm 0.6 \times 10^{-6}$. The non-dimensional velocity profiles for all surfaces under the influence of pressure gradients were presented at 3 stations of 60, 300 and 660 mm, as in the laminar flow discussions, as in Fig. 6. The initial boundary layer parameters of δ (<10 mm), Re_x ($>2.2 \times 10^6$), Re_θ (>1100) and H (<1.5) show that the flow for all cases have turbulent characteristics, which are similar to those of Cheng et al. [22] for the flat surface and Kestoras and Simon [19] for the concave surface. These boundary layer parameters, towards the downstream (x = 660 mm), became 1400, 2000 and 2250 for Re_θ and 1.3, 1.5 and 1.6 for H in case of concave, flat and convex surfaces respectively, which are in agreement with those of Volino and Simon [7]. The thinner turbulent boundary layers, at the strongest favourable pressure gradient of 0.6×10^{-6}, is similar to that of Cheng et al. [22] and are more apparent towards the end of the test section (Fig. 6), with Re_θ and H values of 1300, 1400 and 1750 and of 1.60, 1.70 and 1.90 on concave, flat and convex surfaces respectively. Even the highest favourable pressure gradient of $k = 0.6 \times 10^{-6}$ was not sufficient to relaminarize the flow so that velocity

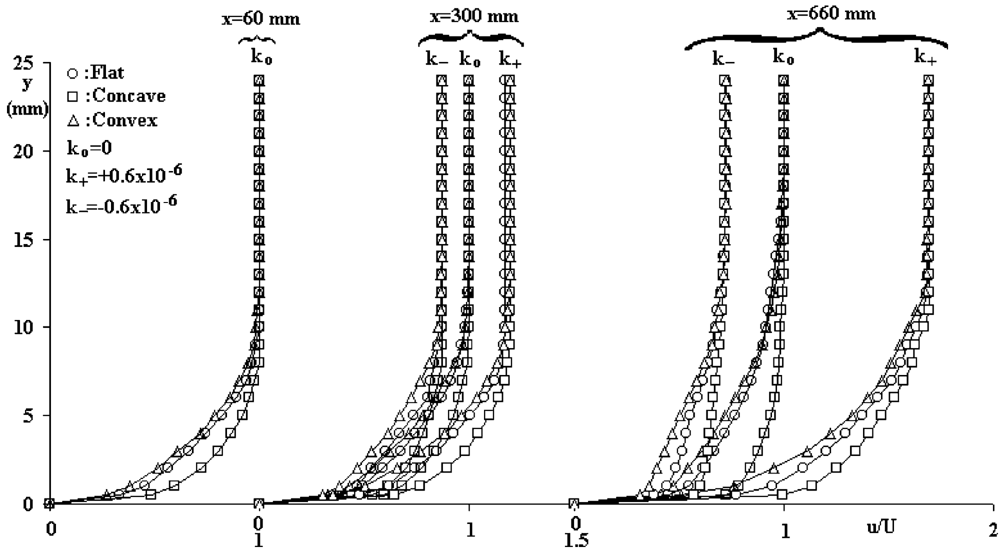

Fig. 6. Streamwise variation of turbulent velocity profiles with k = 0 and $\pm 0.6 \times 10^{-6}$

profiles showed turbulent flow characteristics in all measurement stations. The boundary layer thickness at the adverse pressure gradient of $k = -0.4 \times 10^{-6}$ increased particularly at the last measuring stations. The turbulent boundary layer on the convex surface was seen to be more resistant to adverse pressure gradient than laminar flow and no separation took place. Higher Re_θ and H values account for all surfaces than near zero pressure gradient. The lowest adverse pressure gradient of -0.6×10^{-6}, with 25% reduction in core flow velocity caused further increases in δ for all surfaces, which is similar to that of Rivir et al. [16] for flat surface and of So and Mellor [25] for concave surface and of Webster et al. [18] for convex surface. These encounter higher boundary layer parameters of Re_θ and H and more resistant turbulent flow than that of $k = -0.4 \times 10^{-6}$ case over all surfaces.

The streamwise variation of turbulent Stanton numbers of Fig. 7, in the presence of favourable pressure gradients, exhibit that concave surface has the highest and convex surface has the lowest values, as in the previous case of laminar flow. The experimental results are also compared with the turbulent correlation of Eq. (3).

$$St = 0.03 Re_x^{-0.2} Pr^{0.4} \left(1 - (x_l/x)^{0.9}\right)^{1/9} \quad (3)$$

For near zero pressure gradient case, the measured turbulent St values rose by a factor of 1.3 for concave, 1.6 for flat and 1.7 for convex surfaces, towards the downstream, with respect to laminar flow values. The turbulent St augmentation is in good agreement with Rivir et al. [16], Turner et al. [23] and Taylor et al. [14], but comparable to Mayle et al. [24] and Ligrani and Hedlung [20]. On the other hand concave and convex wall Stanton numbers were 8% higher and 4% lower at initial stations and 30% higher and 25% smaller at last stations, than flat plate values.

Since the favourable pressure gradient of $k = 0.4 \times 10^{-6}$ has no distinct effect on the initial station velocity profiles and on the corresponding boundary layer parameters of Re_θ and H, initial Stanton numbers remained almost unchanged (close to those of near zero pressure gradient). As shown in Fig. 7, a small amount of augmentation in St,

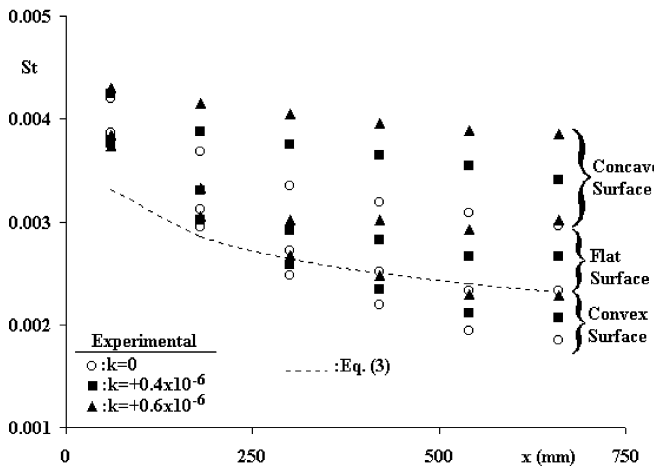

Fig. 7. Streamwise variation of Stanton numbers in turbulent flow with favourable pressure gradients

such as 15% for concave, 14% for flat and 12% for convex, have been recorded towards downstream above zero pressure gradient values. These results are consistent with the convex surface results for mild acceleration of Turner et al. [23], who reported 7.5% increase in turbulent flow. The flat plate Stanton numbers are 28% below concave wall and 21% above convex wall, as predicted in the earlier case.

The pressure gradient of 0.6×10^{-6} caused a further increase in St values on the three surfaces, such as flat surface values are 27% below the concave and 24% above the convex values. As in the mild pressure gradient case, the strongest pressure caused St to increase by 30%, 29% and 24% for concave, flat and convex walls, above near zero pressure gradient values. Measurements showed that heat transfer coefficients increased with acceleration both in laminar and turbulent flows, which is not in good agreement with Umur and Karagöz [8], who showed turbulent St to decrease with acceleration, unlike laminar flows.

The adverse pressure gradient of -0.4×10^{-6} resulted in thicker boundary layers, reduced skin friction and the

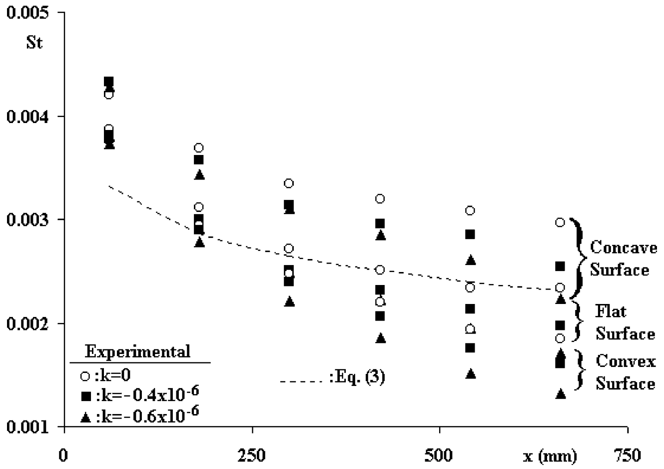

Fig. 8. Streamwise variation of Stanton numbers in turbulent flow with adverse pressure gradients

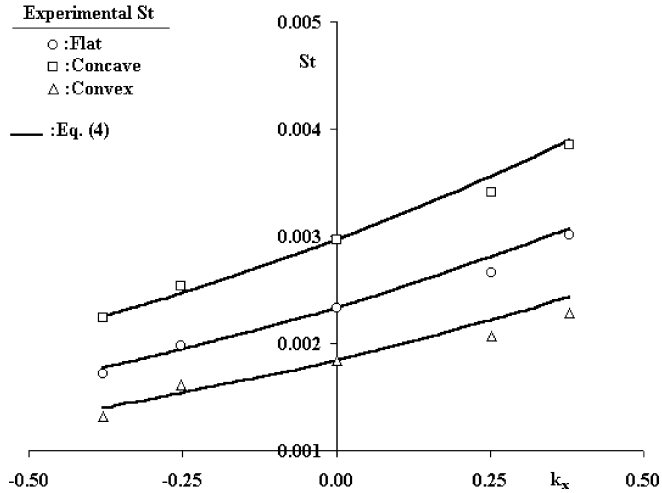

Fig. 9. Turbulent flow Stanton numbers versus k_x

corresponding St as seen in Fig. 8. St decreased by 14% for concave, 15.5% for flat and 12.5% for convex surface with respect to near zero pressure gradient. Flat surface St are 29% below the concave and 18% above the convex values.

The streamwise heat transfer variations with k of -0.6×10^{-6} show similar characteristics to those of $k = -0.4 \times 10^{-6}$. St decreased up to 25% for concave, 27% for flat and 29% for convex with respect to no pressure gradient. Flat surface heat transfer values are 25% higher than the convex surface and 30% lower the concave surface values. The variation in Stanton number with $k = -0.6 \times 10^{-6}$ is more pronounced than that of $k = -0.4 \times 10^{-6}$, that might be contributed to the more influence of higher adverse pressure gradient in turbulent flows.

As for the laminar case the new equation of 4, applicable for three surfaces and for the complete set of favourable and adverse pressure gradients, was developed by modifying Eq. (2).

$$St_p = St_o \exp(0.7k_x) \tag{4}$$

St values are also plotted with respect to k_x for the three surfaces in Fig. 9, together with Eq. (4). The results showed that accelerating flows caused St to increase and decelerating flows to decrease, which is in good agreement with Eq. (4). Flat surface St are above that of the convex by 25% and below concave values by 30% for the streamwise pressure gradient of $k_x = -0.47$ ($k = -0.6 \times 10^{-6}$). On the other hand the strongest favourable streamwise pressure gradient of $k_x = 0.47$ ($k = 0.6 \times 10^{-6}$) showed similar trends like 24% increase (flat-convex) and 27% decrease (flat-concave). Eq. (4) is consistent with all measured values with a precision of ±4% and can be used in the range of $-1.0 \leq k_x \leq 1.0$.

4
Conclusion

Flow and heat transfer measurements, under the influence of favourable and adverse pressure gradients, were carried out on flat, concave and convex surfaces. It was found that the favourable pressure gradients and concave curvature caused thinner boundary layers, which corresponds to an augmentation of heat transfer coefficients both in laminar and turbulent flows. The concave surface destabilised the flow and enhanced heat transfer, while the convex surface stabilised the flow and decreased heat transfer rates. Convex curvature and adverse gradients produced thicker boundary layers and corresponding lower skin friction coefficients and Stanton numbers. The laminar flow with the lowest pressure gradient of $k_x = -0.47$ was found to be more vulnerable than the same turbulent flow condition.

While concave surface increased St up to 90% in laminar and 30% in turbulent flows, convex surface decreased St by 35% in laminar and by 25% in turbulent flows with respect to the flat plate values. Acceleration caused Stanton number to rise up to 35% on concave, 28% on flat and 16% on convex surfaces in laminar flows, and 30% on concave, 29% on flat and 24% on convex surfaces in turbulent flows. Deceleration reduced St up to 26% on concave, 31% on flat and 22% on convex surfaces in laminar flows, and 25% on concave, 27% on flat and 29% on convex surfaces in turbulent flows. The results showed that the effect of surface curvature on heat transfer became more pronounced than pressure gradients both in laminar and turbulent flows. The new equations of 2 in laminar and of 4 in turbulent flows were successfully used to estimate the Stanton numbers, as functions of k_x, within an accuracy of less than $\mp 4\%$.

References

1. Abu-Ghannam BJ; Shaw H (1980) Natural transition of boundary layers-the effects of turbulence, pressure gradient and flow history. Mech Eng Sci 22: 213–228
2. Crane RI; Sabzvari J (1989) Heat transfer visualization and concave-wall laminar boundary layers. J Turbomachinery-Transactions ASME 111: 51–56
3. Umur H (1994) Concave wall heat transfer characteristics with longitudinal pressure gradients and discrete wall jets. JSME Int J 37: 403–412
4. Gostelaw JP; Blunden AR; Walker GJ (1994) Effects of free-stream turbulence and adverse pressure gradients on boundary layer transition. J Heat Transfer-Transactions ASME 116: 392–404
5. Zhang DH; Winoto SH; Chew YT (1995) Measurement in laminar and transitional boundary-layer flows on concave surface. Int J Heat Fluid Flow 16: 88–98

6. Zhou D; Wang T (1996) Combined effects of elevated free-stream turbulence and streamwise acceleration on flow and thermal structures in transitional boundary layers. Exp Thermal Fluid Sci 12: 338–351
7. Volino RJ; Simon TW (1997) Boundary layer transition under high free-stream turbulence and strong acceleration conditions: part 2-turbulent transport results. J Heat Transfer-Transactions ASME 119: 427–432
8. Umur H; Karagoz I (1999) An investigation of external flows with various pressure gradients and surfaces. Int Com Heat Mass Trans 26: 411–419
9. Sturgis JC; Mudawar I (1999) Single-phase heat transfer enhancement in a curved, rectangular channel subjected to concave heating. Int J Heat Mass Trans 42: 1255–1272
10. Wright L; Schobeiri MT (1999) The effect of periodic unsteady flow on aerodynamics and heat transfer on a curved surface. J Heat Transfer-Transactions ASME 121: 22–33
11. Umur H (2000) Flow and heat transfer with pressure gradients, Reynolds number and surface curvature. Int Com Heat Mass Trans 27: 397–406
12. Muck KC; Hoffman PH; Bradshaw P (1985) The effect of convex surface curvature on turbulent boundary layers. J Fluid Mech 161: 347–369
13. Wang T; Simon TW (1987) Heat transfer and fluid mechanics measurements in transitional boundary layers on convex-curved surfaces. J Turbomachinery-Transactions ASME 109: 443–451
14. Taylor RP; Coleman HW; Hosni MH; Love PH (1989) Thermal boundary condition effects on heat transfer in the turbulent incompressible flat plate boundary layer. Int J Heat Mass Trans 32: 1165–1174
15. Plesniak MW; Mehta RD; Johnston JP (1994) Curved two-stream turbulent mixing layers: three dimensional structure and streamwise evolution. J Fluid Mech 270: 1–50
16. Rivir RB; Johnston JP; Eaton JK (1994) Heat transfer on a flat surface under a region of turbulent separation. J Turbomachinery-Transactions ASME 116: 57–62
17. Inagaki K; Aihara Y (1995) An experimental study of the transition region of the boundary layer along a concave wall. European J Mech B/Fluids 14: 143–168
18. Webster DR; Degraaff DB; Eaton JK (1996) Turbulence characteristics of a boundary layer over a two-dimensional bump. J Fluid Mech 320: 53–69
19. Kestoras MD; Simon TW (1997) Turbulent transport measurements in a heated boundary layer: combined effects of free-stream turbulence and removal of concave curvature. J Heat Transfer-Transactions ASME 119: 413–419
20. Ligrani PM; Hedlung CR (1998) Transition to turbulent flow in curved and straight channels with heat transfer at high Dean numbers. Int J Heat Mass Trans 41: 1739–1748
21. Cebeci T; Bradshaw P (1984) Physical and computational aspects of convective heat transfer. Springer-Verlag, New York
22. Cheng KC; Obata T; Gilpin RR (1988) Buoyancy effects on forced convection heat transfer in the transition regime of a horizontal boundary layer heated from below. J Heat Transfer-Transactions ASME 110: 596–603
23. Turner AB; Hubbe-Walker SE; Bayley FJ (2000) Fluid flow and heat transfer over straight and curved rough surfaces. Int J Heat Mass Trans 43: 251–262
24. Mayle RE; Blair MI; Kopper FG (1979) Turbulent boundary layer heat transfer on curved surfaces. J Heat Transfer-Transactions ASME 101: 521–525
25. So RM; Mellor GL (1975) Experiment on turbulent boundary layers on a concave wall. Aeronaut Quart 26: 25–40